

# USING THE CONE CALORIMETER TO DEVELOP A DETAILED MODEL OF CARPET FOR FLAMMABILITY STUDIES

Kathryn M. Butler<sup>\*</sup>, K. Ranjan Samant<sup>†</sup>, John R. Shields<sup>\*</sup>

<sup>\*</sup> National Institute of Standards and Technology, Gaithersburg, MD, USA

<sup>†</sup> E.I. DuPont de Nemours and Company, Wilmington, DE, USA

## ABSTRACT

A fundamental mathematical model of carpet is needed for studying the impact of component materials and thicknesses on tests that measure flammability. Of particular interest is the ASTM E648 radiant panel test, which is used to qualify floor coverings for commercial installations. The flammability characteristics of carpet in the cone calorimeter are expected to relate closely to carpet behavior in the ASTM E648 test. Accordingly, the combination of materials and their properties were sought that produces a match between cone calorimeter modeling and experiment. Careful measurements were taken from cone tests performed on broadloom style carpet composites for three types of fiber, on fiber plus primary backing alone, and on samples with adhesive plus one or both backings. Steps were taken to overcome the challenge of securing thin materials that curl and shrink during testing. This combination of tests enabled the determination of mass fraction, char yield, and heat of combustion for each individual component as well as capturing critical information such as time to ignition and effective heat of combustion for whole samples. These values can be used as input parameters for a cone calorimeter model to compare with experimental results.

A simple transformation was found that collapses plots of heat release rate (HRR) for cone heat fluxes between 15 kW/m<sup>2</sup> and 35 kW/m<sup>2</sup> into a single curve for each carpet type. Broadloom style carpet is neither thermally thick nor thermally thin. As with many materials, however, both peak heat release rate (PHRR) and inverse time to ignition are linear functions of cone heat flux. The recognition that the inverse time to PHRR is also a linear function of cone heat flux results in the universal curve. This behavior may permit a more simplified approach to modeling more complex problems.

## INTRODUCTION

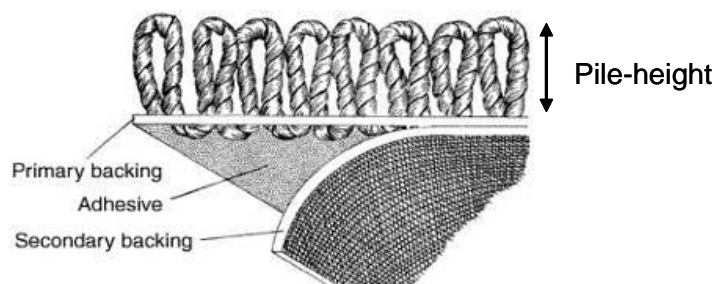
Floor coverings such as carpet can potentially contribute to fire growth in buildings by spreading flame through corridors and exit ways. In order to be accepted for use in commercial buildings, carpets must pass the ASTM E648 standard test<sup>1</sup> that assesses the propensity of floor coverings to spread flames when subjected to a thermal radiant flux. This test method represents a scenario in which a floor covering is exposed to the thermal radiation from a fully developed fire in an adjacent room. A carpet undergoing this test is subjected to a heat flux that varies smoothly with distance over the sample due to a radiant panel mounted at an angle. The sample is ignited, and the flame spreads towards the lower flux end of the sample. After the test, the distance from the edge of the burned sample to the point of flame extinction is measured and converted to a critical radiant heat flux (CRF) that is necessary to support the spread of flames over the surface of the material.

A model of the ASTM E648 test would improve the capability to design carpets that meet flammability requirements. Modern computational tools have a good track record in modeling fire in the gas phase in complex geometries; however, the treatment of condensed phase burning is not as well-developed. Because of the nature of its materials and construction, carpet is a particularly challenging material to model. The thermal transport through and flame spread over the carpet sample depend on the physical

and chemical details of its composition. As the carpet heats and burns, it may char, melt, and undergo chemical changes. The material properties needed for input to the model may vary with temperature, and it is difficult to extrapolate values measured in normal test conditions to values at fire temperatures. The cone calorimeter test is a bench-scale test that studies small (10 cm x 10 cm) samples as they burn under exposure to a uniform radiant heat flux. Outputs include mass loss rate and heat release rate as a function of time. The cone calorimeter provides a simple analogue to the ASTM E648 test. If a model of carpet undergoing the cone calorimeter test provides good agreement with experiment for a range of heat flux levels, it will be useful to examine whether the same input parameters would be successful in a model of the ASTM E648 test.

Broadloom carpet construction is illustrated in Figure 1. This carpet consists of a pile with loose fibers or loops. The fiber is woven through a fabric called the primary backing. A layer of adhesive bonds the primary backing to a layer of fabric called the secondary backing, which provides stiffness and protects the weave.

Figure 1. Broadloom carpet construction



This paper describes the cone calorimeter experiments performed on carpet samples, including the techniques used to minimize the difficulties with these thin samples. Photos of residues and mass loss and heat release rate (HRR) plots are presented. A transformation is shown that collapses the HRR plots at various heat fluxes into a single curve for each fiber type. The determination of parameter values for use in modeling is briefly described, followed by the cone calorimeter modeling approach and results.

## CONE CALORIMETER EXPERIMENTS

Three types of carpet fiber were selected for this set of experiments: polypropylene (PP), Nylon 6,6 (N66), and polytrimethylene terephthalate (PTT). Fully assembled composite carpet samples were manufactured by weaving the carpet fiber in a level loop design through a PP primary backing, then attaching the fiber layer with styrene butadiene latex adhesive to a PP secondary backing, as illustrated in Figure 1. All three carpet fibers were woven with the same fabric areal density of 0.814 kg/m<sup>2</sup> (24 oz/sq yd). To separate the contribution to flammability from each component, samples were created that consisted of the composite carpet, the fiber layer (fibers and primary backing) only, and an adhesive layer applied on the secondary backing alone or between the two backings. Standard carpet manufacturing methods were used for composite carpets and fiber layers. Applying the adhesive to backings without fiber was an unusual operation, and adhesive layer thickness for these samples was more variable than for the standard composite carpet samples. The sample types are listed in Table 1, with abbreviated names that will be used throughout the paper.

Composite carpets were tested at cone heating levels of (35, 25, 20, and 15) kW/m<sup>2</sup>. This range was selected as representing the heat flux levels encountered by a carpet subjected to the ASTM E648 test. The radiant panel is designed to provide up to 12 kW/m<sup>2</sup> to the carpet sample. Additional heat is provided by flame feedback and the heating of the test apparatus. The flame flux for nylon and PP have been estimated as 30 kW/m<sup>2</sup> and 14 kW/m<sup>2</sup> respectively.<sup>2</sup> A model of the ASTM E648 test estimated maximum heat flux to the burning carpet on the order of 50 kW/m<sup>2</sup>, equivalent to a cone calorimeter heat flux of 35 kW/m<sup>2</sup> plus 15 kW/m<sup>2</sup> flame feedback. Lower values of cone heat flux serve to explore

the behavior of carpets near the critical value necessary to maintain burning, the central focus of the ASTM E648 test.

Table 1. Carpet sample types

Composite carpet samples		Fiber layer samples		Backing + Adhesive Samples	
PP-24_C	PP fiber, 0.814 kg/m <sup>2</sup>	PP-24_F	PP fiber, 0.814 kg/m <sup>2</sup>	S+A	Secondary + Adhesive
N66-24_C	N66 fiber, 0.814 kg/m <sup>2</sup>	N66-24_F	N66 fiber, 0.814 kg/m <sup>2</sup>		
PTT-24_C	PTT fiber, 0.814 kg/m <sup>2</sup>	PTT-24_F	PTT fiber, 0.814 kg/m <sup>2</sup>	P+S+A	Primary + Secondary + Adhesive

Fiber layers and backing plus adhesive samples were tested at 35 kW/m<sup>2</sup> only. For all samples, three trials were run under each condition.

### Preparation

The 10 cm x 10 cm square cone calorimeter samples were cut from carpet rolls and conditioned for at least three days. The carpet samples were thinner than recommended for standard cone use, and problems were apparent in the first test attempts. During heating, the unrestrained composite samples pulled in from the edges and clumped in the center of the holder as they burned. The fiber layer samples were lightweight enough to allow the aluminum foil holding the sample to rise in the center as it heated. As a result, the melt from the fibers flowed to the sides, and burning occurred only around the edges of the holder.

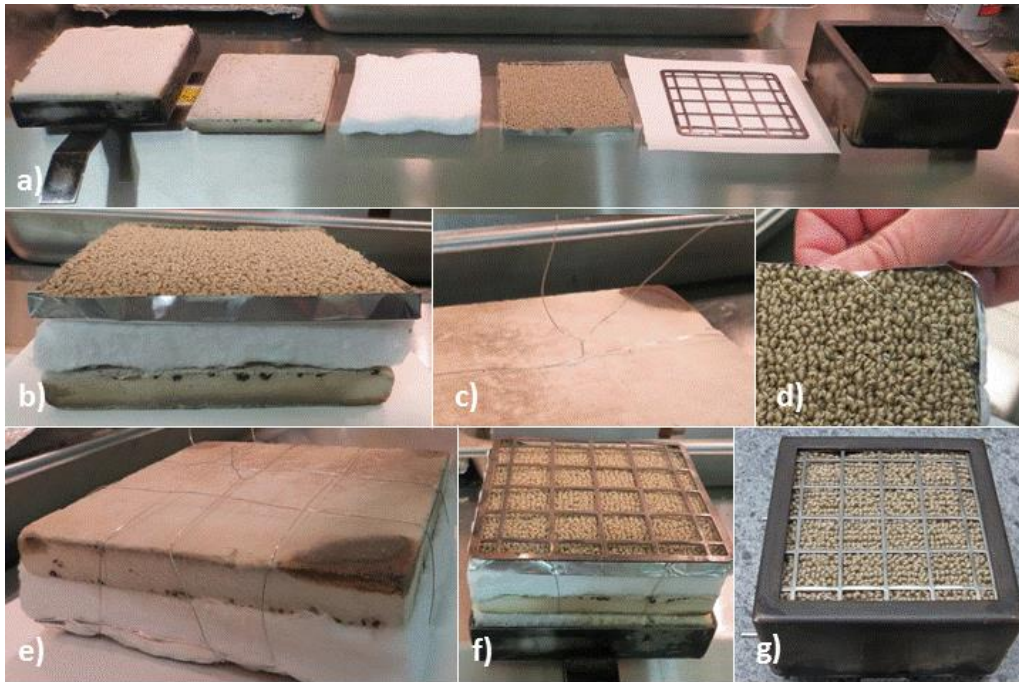
For the composite carpets, the problems were resolved by the procedure for sample mounting and assembly shown in Figure 2. Figure 2(a) shows the components used in sample assembly. From left to right are the bottom half of the sample holder containing sufficient layers of Kaowool<sup>†</sup> to firmly pack the final assembly, a 13 mm thick marinite board, a 13 mm thick layer of fresh Kaowool, the carpet sample wrapped in aluminum foil, a flat steel grid recommended for use with certain cone calorimeter samples such as and the top half of the specimen holder. The flat grid is similar to the wire grid recommended for cone calorimeter use with intumescent samples<sup>3</sup> and for fabrics.<sup>4</sup> It was found to be better than the wire grid at restraining the carpet in all directions as it heated and shrank.

To assemble, first the marinite board, fresh Kaowool, and carpet sample are put together as in Figure 2(b). A 1 m long Nichrome wire is placed along the centerline of the carpet, and the assembly is turned upside-down as in Figure 2(c). The wire is wrapped around the assembly and twisted near one end. The long end of the wire is placed along the edge 20 mm to 25 mm from the corner and wrapped sequentially around each corner of the sample as shown in Figure 2(d). The aluminum foil must be bent toward the sample so that it continues to retain the melt as the sample burns. Figure 2(e) shows the final appearance of the bottom of the sample assembly, after the wire is tied off. The assembly is then arranged on the Kaowool layers within the lower half of the specimen holder with the mesh laid on top as shown in Figure 2(f). Figure 2(g) shows the final specimen after the top of the specimen holder was fixed in place. Note that the holder and steel grid cover part of the sample. The area exposed directly to the heat flux from the cone and the flame is reduced to 0.00884 m<sup>2</sup> from the 0.01 m<sup>2</sup> of the full sample. Beneath the metal edges and bars, the heat transfer is conductive rather than radiative. As the fiber melts, however, many areas of the sample lose contact with the grid, and the sample burns more or less uniformly. Calculations therefore assume the entire 0.01 m<sup>2</sup> area of the sample.

The backing and adhesive samples were also restrained using this technique.

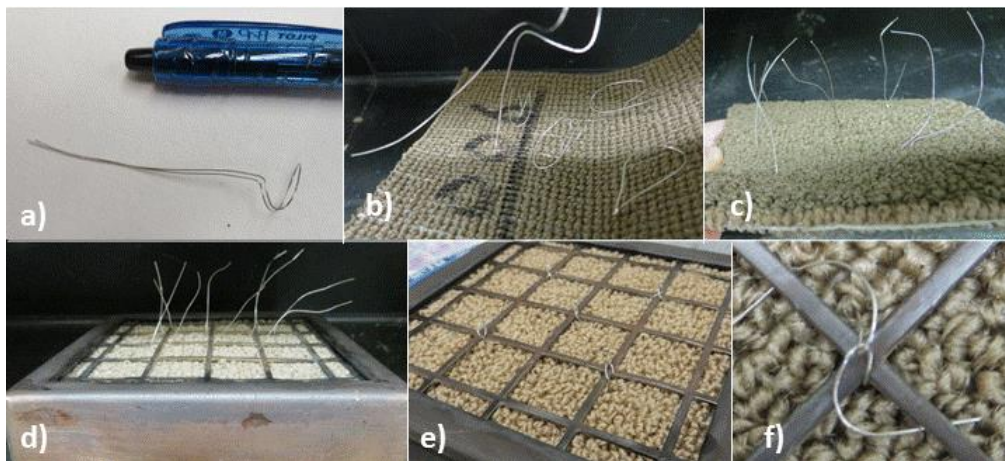
<sup>†</sup> Mention of commercial materials, equipment, products, or services in this paper does not imply approval or endorsement by NIST, nor does it imply that such materials, equipment, products, or services are necessarily the best available for the purpose.

Figure 2. Preparation of composite carpet samples for cone calorimeter



For fiber layer samples, the bulging of the aluminum foil holder and the subsequent melt flow required the development of a new approach. Figure 3 shows an approach that keeps the aluminum foil sufficiently flat that the polymer melt remains uniformly distributed over the surface. For each sample, five mechanical springs are created from 15-cm lengths of Nichrome wire. The wires are folded in two and formed over the thumb to create the device shown in Figure 3(a). The ends of the springs are pressed through adjacent holes in the fiber mesh on the back side of the sample in five locations roughly corresponding to intersections of the bars in the flat steel grid. The straight parts of the wires are drawn through the fiber layer as shown in Figure 3(b), with Figure 3(c) showing the wires when the sample is turned right-side up. The sample is then placed on the aluminum foil. When placing the flat steel grid on top as in Figure 3(d), each of the five pairs of wires is pulled through such that one wire is at one corner of the intersecting bars and the other is at the opposite corner. The wire pairs are wrapped around the bars as shown in Figure 3(e), and the ends are clipped and folded under the bars as in Figure 3(f). This final step prevents the ends of the wires from moving and touching the igniter during the test. After the cone tests, the Nichrome wire was found to have retained its springiness.

Figure 3. Preparation of fiber layer samples for cone calorimeter



### Cone calorimeter tests

Cone calorimeter testing was carried out on the NIST research cone calorimeter according to the procedures from the ISO 5660-1 standard.<sup>5</sup> The mass of each sample was measured before and after placement in the aluminum foil holder, and the residue plus aluminum foil were measured after the test. Each test was videotaped.

*Carpet composites.* Figure 4 shows the samples after burning for carpet composites with identical fiber densities. Images are arranged left to right from highest to lowest cone heat fluxes. Carpets burned differently depending on the fiber material. With PP fibers, the carpet shrank and pulled away from the sides of the holder, as indicated by the bare spots in the images along the top row. The PP fibers were observed to liquefy well before ignition, and bubbling was observed throughout the test. When the N66 carpet samples in the center row were heated at 35 kW/m<sup>2</sup> or 25 kW/m<sup>2</sup>, horizontal shrinkage primarily occurred along one dimension, causing the carpet to try to fold like a fan. Cone heat flux of 20 kW/m<sup>2</sup> was found to be a marginal case; for two samples the burning was uniform, and for another two samples flames occurred in one spot only and extinguished without igniting the rest of the sample. No trials at 15 kW/m<sup>2</sup> supported continuous burning. Along the bottom row, PTT carpets left a white residue with black edges that widened as cone heat flux decreased. The samples experienced little shrinkage, and the residues were flat and powdery.

To test the state of the fiber layer during combustion, a final set of PP, N66, and PTT composite carpet samples were exposed to 35 kW/m<sup>2</sup> cone heat flux up to the time of ignition for each sample. At this time, the samples were removed from the cone calorimeter and allowed to cool. In all cases, the carpet fibers were fully melted, while the secondary backing at the bottom of the sample, although partially melted, still retained its woven structure.

Figure 4. Residues from composite carpet samples after exposure to range of cone heat fluxes

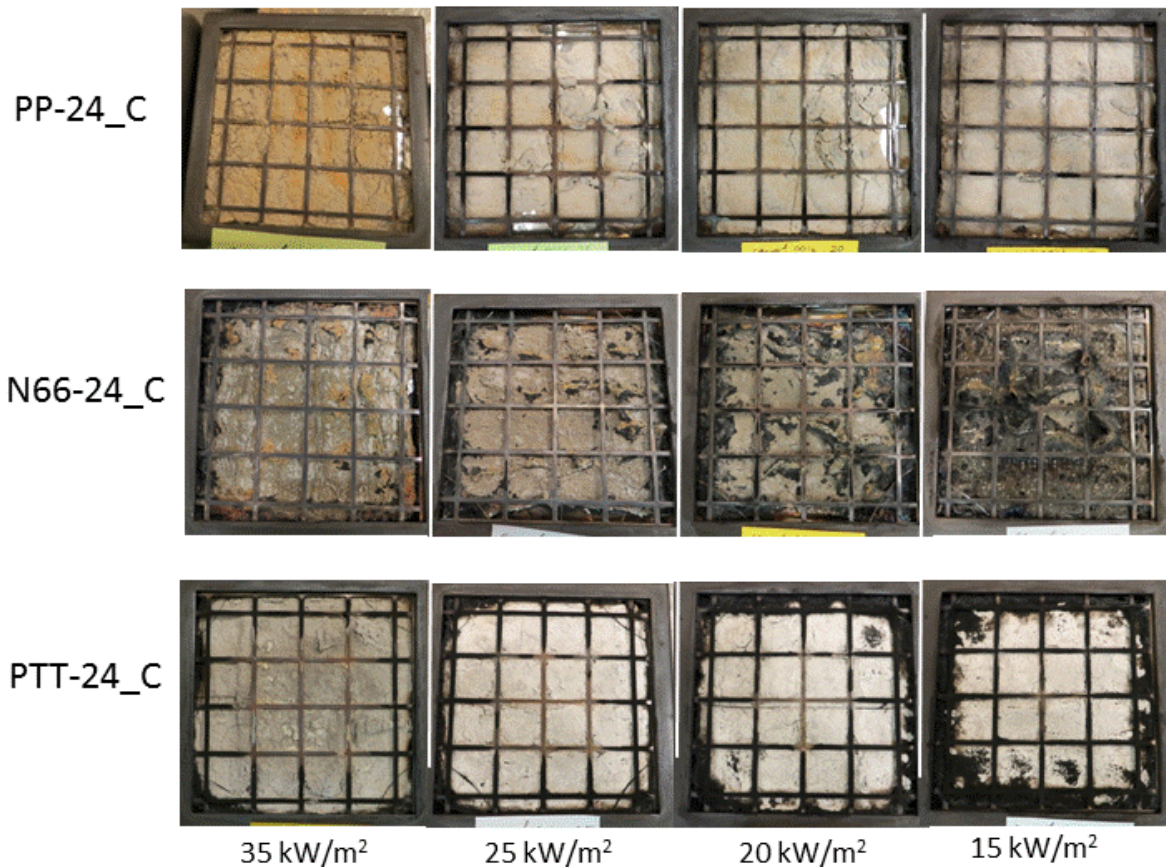
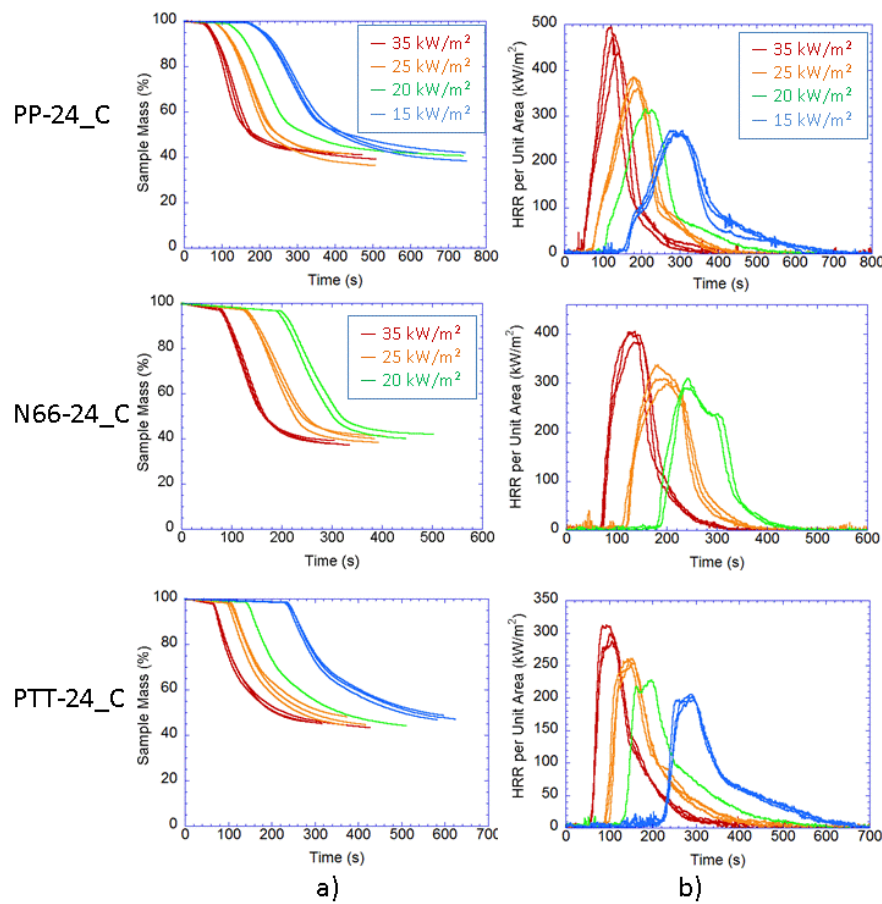


Figure 5 displays plots of relative mass loss and heat release rate (HRR) per unit area as functions of time for the carpet composite samples with identical fabric areal density. Up to three trials were run for each case, indicated by multiple plots of the same color. Despite the messy behavior of the carpet samples during the tests, the time-dependent data agreement among trials was good, generally within  $\pm 5\%$ . The plots for  $15\text{ kW/m}^2$  have been left out for N66 carpets because these samples did not burn uniformly at this cone flux. The differences in fiber type and in cone heat flux result in differences in mass loss rate, in peak heat release rate (PHRR), in plot shape, and in the timings for ignition, PHRR, and extinction. However, the final sample mass as a fraction of the initial mass is similar for all cases at about  $40\%$ . The tests on fiber layers will show that the char yield of PP is zero, which suggests that the primary source of residue for these carpets is the adhesive, the only material remaining for PP-24\_C.

Figure 5. Composite carpet samples: Dependence on cone heat flux for a) mass loss and b) HRR per unit area vs. time



*Fiber layers.* Typical residues from the fiber layer samples after cone tests at  $35\text{ kW/m}^2$  are shown in Figure 6, with mass loss rate and HRR plots in Figure 7. These samples consist of fiber woven through the PP primary backing. For PP fibers, all samples combusted completely, leaving only the aluminum foil base and spring offsets below the steel grid. This is consistent with the zero char yield expected from PP. The melt was low viscosity and flowed freely over the aluminum foil, bubbling constantly during the test. Near the end of the test, smoking was observed from the corners of the sample, indicating that some of the material had leaked out and dripped down into the Kaowool insulating layers. This problem is reflected in the high variability among trials for mass loss rate and HRR plots shown in Figure 7. To calculate material properties, the char yield from PP fiber layer samples was set to zero, and the value of total heat release was corrected by the fraction of mass that was actually burned.

N66 fiber layers burned relatively uniformly over the surface, leaving black char as shown in Figure 6. Figure 7 shows the high level of consistency from these samples. PTT fiber layer cone tests left a small residue. After the tests, the aluminum foil was degraded and ripped easily during preparation for a second weighing after the test.

Figure 6. Residue from fiber layer samples under 35 kW/m<sup>2</sup> cone heat flux

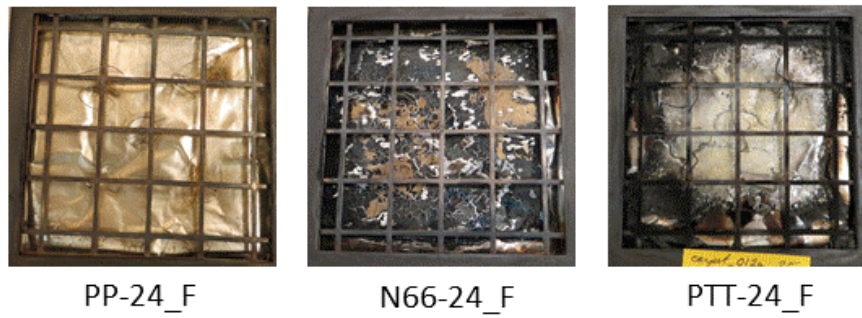
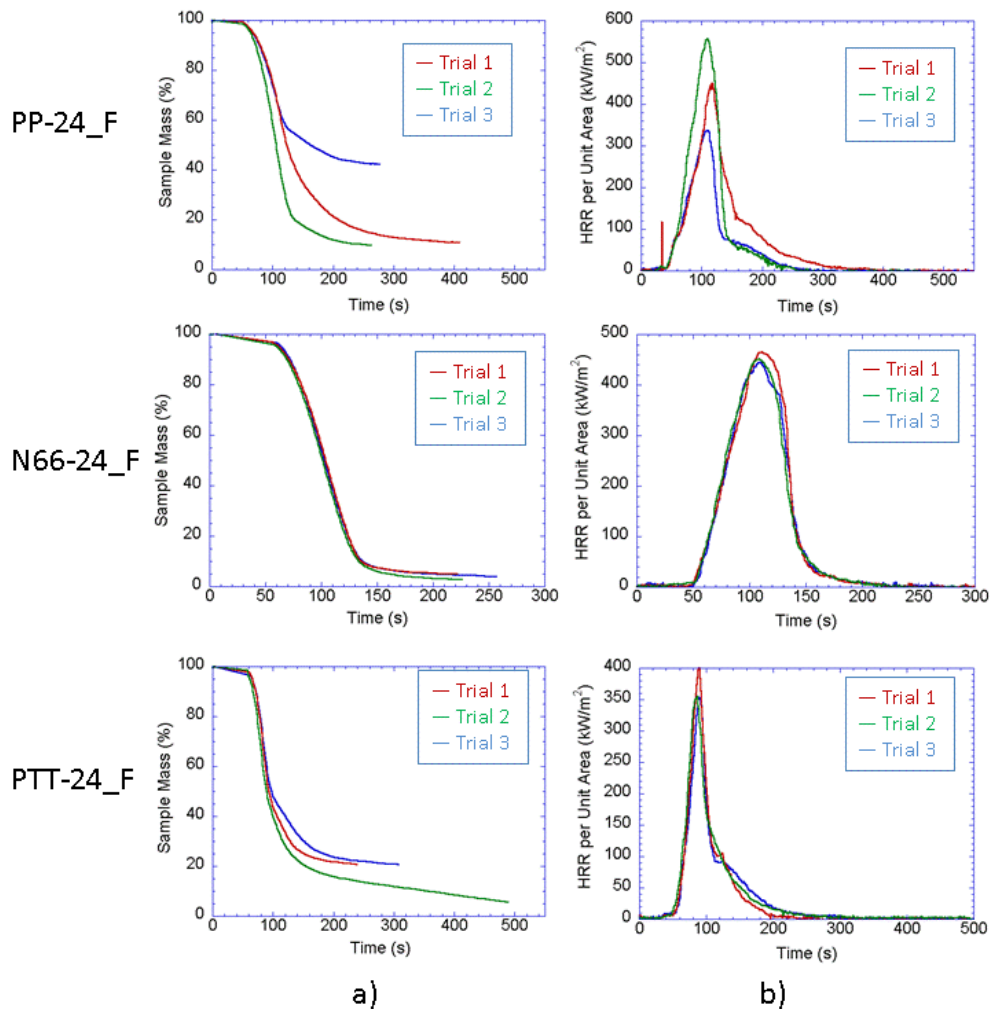


Figure 7. Fiber layer samples under 35 kW/m<sup>2</sup>: a) mass loss and b) HRR per unit area vs. time



*Adhesive plus backings.* Figure 8 shows typical residues from the two sample types without carpet fiber. The secondary backing plus adhesive sample (S+A) kept its original shape without shrinking and burned uniformly. The mass loss plot in Figure 9 shows that nearly 80 % of the mass from this sample was retained, supporting the argument that the adhesive is the major contributor to char yield from carpet samples. The long tails in both mass loss and HRR plots for this sample show the continuing cooking of the char after active burning.

The samples with both backings plus adhesive (P+S+A) behaved quite differently. The floppiness of these samples indicated that the amount of adhesive in these samples was considerably less than that in the S+A sample or the carpet composites. The horizontal shrinkage was significant even with the help of the Nichrome wire wrapping, as shown by the bare edges surrounding the residue in Figure 8. Figure 9 shows the results and degree of variability for these samples.

Figure 8. Residues from adhesive/backing samples under 35 kW/m<sup>2</sup> cone heat flux

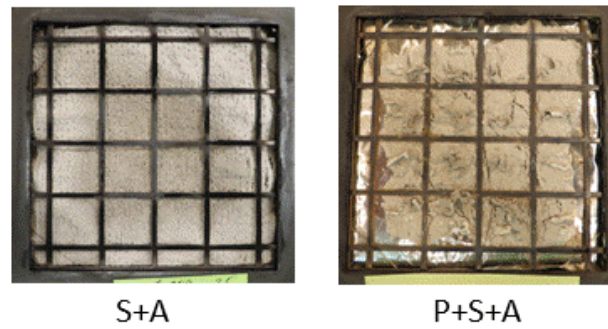
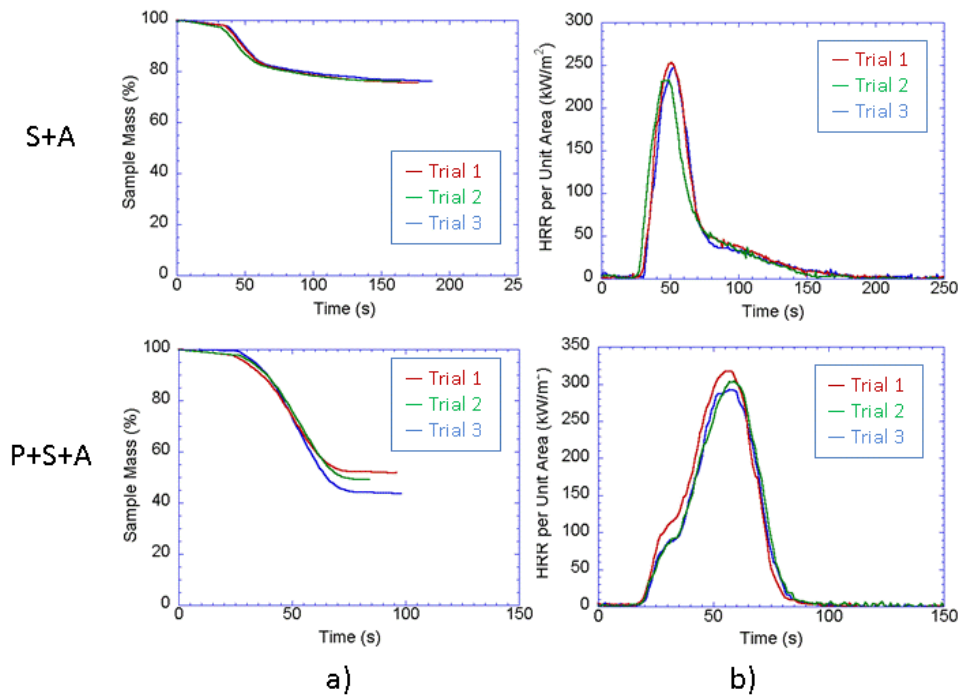


Figure 9. Adhesive/backing samples under 35 kW/m<sup>2</sup>: a) mass loss and b) HRR per unit area vs. time



### Cone calorimeter results

Figure 10 shows the variation of four important measurements with cone calorimeter heat flux for composite carpet samples. Error bars in these plots reflect measurement uncertainties. Uncertainties in HRR due to cone calorimeter instrument and calculation assumptions exceed  $\pm 5\%$ .<sup>6</sup> To incorporate sample and operator variability, standard deviations were calculated at each cone heat flux level for Figure 10(a) and (b). The maximum relative uncertainty for each polymer was selected for the error bars, which extend over two standard deviations (95% confidence level for a normal distribution). For Figure 10(c) and (d), the standard deviation was calculated over all heat fluxes. The minimum relative uncertainty in every plot is bounded at  $\pm 5\%$ .

In Figure 10(a), the inverse time to ignition is found to be linear with cone heat flux for each fiber type. This is consistent with the behavior of thermally thin samples,<sup>7</sup> although since the temperature is not uniform throughout the sample, carpets are not actually thermally thin. Figure 10(b) shows that peak heat release rate is also a linear function of heat flux.

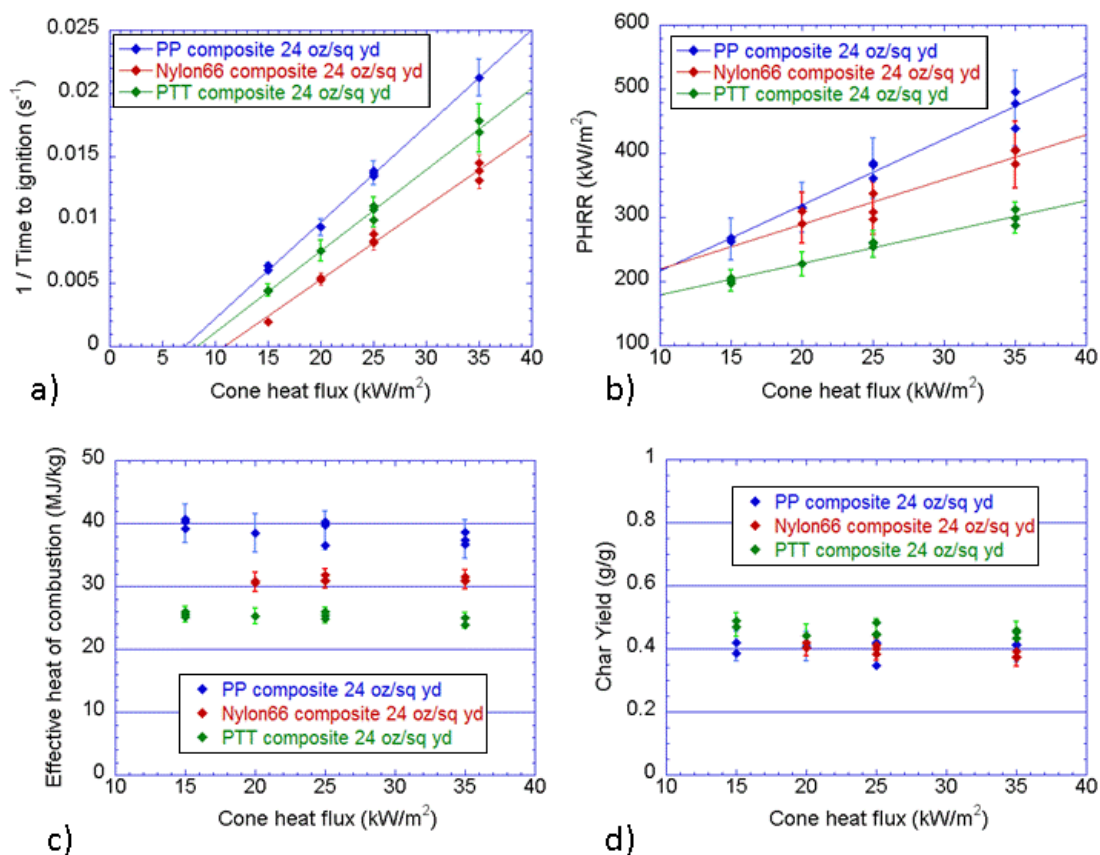
The effective heat of combustion for each carpet sample was determined by dividing the total heat release from ignition to flame-out by the total mass lost. Figure 10(c) indicates that the dependence of the effective heat of combustion on cone heat flux is small. Since the composite samples generally differ only by fiber type, this figure also shows that the ordering of fibers by effective heat of combustion from lowest to highest is PTT < N66 < PP.



The mass of the entire sample was measured both before and after the test. The ratio of final to initial mass is the residue yield, which is used interchangeably with the term char yield within this paper, although inert materials are included in the residue. Figure 10(d) shows that the char yield does not depend strongly on either cone heat flux or fiber type. This indicates that the char is produced primarily by the parts of the composite carpet that are common to all samples. Since the backings are made of PP, which burns without leaving a char, the char yield must be primarily due to the adhesive.

Comparisons of time plots of mass loss rate and heat release rate divided by the heat of combustion were nearly identical and showed that water vapor and other inert gases do not play a role.

Figure 10. Effects of cone calorimeter heat flux on a) inverse time to ignition, b) peak heat release rate, c) effective heat of combustion, and d) char yield for composite carpets



## COLLAPSE OF HRR PLOTS

Similarities in the plots of HRR vs. time for a range of heat fluxes, as shown in Figure 5(b), raised the possibility that a transformation could be found that would allow the plots for each carpet type to collapse into a single plot. If this is the case, a simpler global approach may be possible for more complicated fire problems.

Two time periods are easily obtained from HRR plots: time to ignition and time to PHRR. It has already been determined that inverse time to ignition has a linear relationship with cone heat flux. Plotting inverse time to PHRR as a function of heat flux reveals that this relationship is also linear, as shown for PP-24\_C in Figure 11(a) as an example. A nondimensional time  $\tau$  can now be defined as

$$\tau = \frac{t - t_{ig}}{t_{PHRR} - t_{ig}} = \frac{t - (A + B\dot{q}_c'')^{-1}}{(C + D\dot{q}_c'')^{-1} - (A + B\dot{q}_c'')^{-1}} \quad (1)$$

where  $t$  is time,  $\dot{q}_c''$  is cone heat flux, and (A, B) and (C, D) are linear coefficients for  $t_{ig}$ , and  $t_{PHRR}$  respectively. Times  $t_{ig}$  and  $t_{PHRR}$  are normalized to  $\tau = 0$  and 1 respectively.

Nondimensional heat release rate  $\mathcal{HRR}$  is defined as HRR normalized by PHRR. The linear relationship between PHRR and cone heat flux for PP-24\_C is shown in Figure 11(b) and can be written as:

$$\mathcal{HRR}(\tau) = \frac{HRR(\tau)}{PHRR} = \frac{HRR(\tau)}{(E + F\dot{q}_c'')} \quad (2)$$

where (E, F) are the linear coefficients for PHRR.

Coefficients A-F determined from linear relationships for all composite carpets are given in Table 2. These values assume  $t$  is in units of seconds and both  $HRR$  and  $\dot{q}_c''$  are in  $\text{kW/m}^2$ .

Figure 11. Linear dependencies on cone heat flux for a) inverse time to ignition and time to PHRR and b) PHRR for PP-24\_C

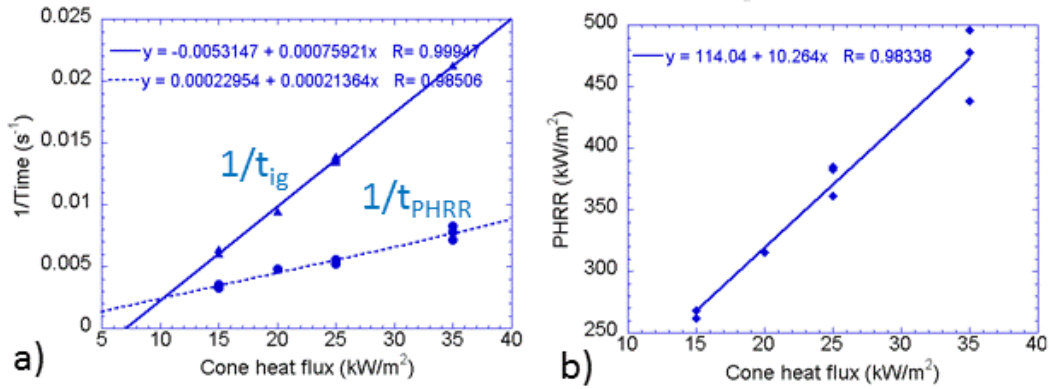


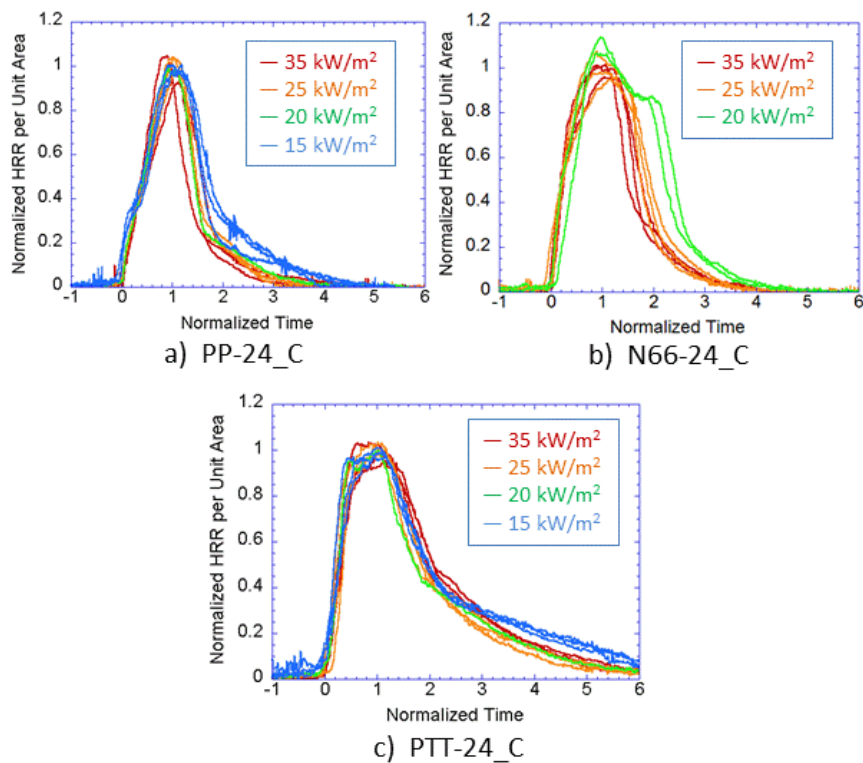
Table 2. Linear coefficients to collapse HRR plots for composite carpet samples

Sample	A*10 <sup>3</sup>	B*10 <sup>3</sup>	C*10 <sup>3</sup>	D*10 <sup>3</sup>	E	F
PP-24_C	-5.31	0.759	0.230	0.214	114	10.3
N66-24_C	-5.84	0.565	-0.479	0.230	103	8.50
PTT-24_C	-5.25	0.641	-1.35	0.322	130	4.93

These transformations for time and HRR convert the HRR plots in Figure 5(b) to the plots in Figure 12(a), (b), and (c) for carpet composites PP-24\_C, N66-24\_C, and PTT-24\_C respectively. Each set of HRR plots collapses onto a single curve. The differences in the tail of the curve for the lowest heat flux in each case may indicate changes in the physics and chemistry as the critical heat flux is approached – further investigation is needed.

To the authors' knowledge, this universal behavior across a range of cone heat fluxes has not previously been reported.

Figure 12. Collapsed plots of normalized HRR vs. time for carpet composite samples.



The intersection point of the lines for inverse time to ignition and inverse time to PHRR in Figure 11 defines a flammability limit (the minimum cone heat flux that supports burning of the carpet sample). At this point, the time to ignition equals the time to PHRR. This is a tighter value than extrapolating the plot of inverse time to ignition to its intersection with the x-axis, where time to ignition is infinite. Table 3 lists the minimum cone heat flux and maximum time to ignition for each composite carpet sample. The flammability limits are consistent with the results that PP and PTT carpet samples burned uniformly in cone tests at 15 kW/m<sup>2</sup> while N66 samples did not achieve sustained combustion at this low heat flux level.

Table 3. Flammability limits by fiber and fiber weight

Sample	Minimum cone heat flux (kW/m <sup>2</sup> )	Maximum time to ignition (s)
PP-24_C	10.6	388
N66-24_C	16.0	314
PTT-24_C	12.2	386

## CONCLUSIONS

Cone calorimeter tests on carpet samples required special handling to obtain uniform burning with minimal shrinkage in area. Using wire to wrap the sample with its Kaowool and marinite base and covering the sample with a flat metal grid kept composite samples and samples with adhesive plus backings in place. A new method was developed to manage fiber layer samples that melted completely. For these samples, springs were devised to keep the aluminum holder flat and limit melt flow. Given the difficulties with these carpet samples, results were surprisingly repeatable.

Plots of HRR as a function of time at cone heat flux levels from 15 kW/m<sup>2</sup> to 35 kW/m<sup>2</sup> were reducible to a single curve for each type of composite carpet. This was accomplished by a simple set of transformations derived from linear relationships with cone heat flux for PHRR, inverse time to ignition, and inverse time to PHRR. This finding suggests the possibility of a universal treatment of HRR in modeling applications. To test this, further exploration of behavior is needed at both higher and lower cone heat flux levels.

## ACKNOWLEDGMENTS

The authors would like to thank colleagues at NIST and at DuPont for their invaluable help with planning, experiments, and analysis. This work was funded by E.I. du Pont de Nemours and Company under CRADA number CN-13-0027.

## REFERENCES

- <sup>1</sup> ASTM E648-04, Standard test method for critical radiant flux of floor-covering systems using a radiant heat energy source.
- <sup>2</sup> Babrauskas, V., 2002, Heat release rates, *The SFPE Handbook of Fire Protection Engineering* (3<sup>rd</sup> ed.), Chapter 3-1, National Fire Protection Association, Inc.
- <sup>3</sup> Twilley, W.H. and Babrauskas, V., 1988, User's Guide for the Cone Calorimeter, NBS Special Publication 745, National Bureau of Standards.
- <sup>4</sup> Nazaré, S., Kandola, B., and Horrocks, A. R., 2002, Use of Cone Calorimetry to Quantify the Burning Hazard of Apparel Fabrics, *Fire and Materials* 26:191-199.
- <sup>5</sup> ISO 5660-1:2002, Reaction-to-fire tests – Heat release, smoke production and mass loss rate – Part 1: Heat release rate (cone calorimeter method).
- <sup>6</sup> Enright, P.A. and Fleischmann, C.M., 1999, Uncertainty of Heat Release Rate Calculation of the ISO5660-1 Cone Calorimeter Standard Test Method, *Fire Technology* 35(2): 153-169.
- <sup>7</sup> Delichatsios, M.A., 2000, Ignition times for thermally thick and intermediate conditions in flat and intermediate geometries, *Fire Safety Science – Proceedings of the Sixth International Symposium*, pp. 223-244.